Eur. Phys. J. C 49, 281–286 (2007)
DOI 10.1140/epjc/s10052-006-0128-z

THE EUROPEAN PHYSICAL JOURNAL C

Regular Article – Theoretical Physics

Charged particle multiplicities in $A+A$ and $p+p$ collisions in the constituent quarks framework

R. Nouicer[a]

Brookhaven National Laboratory, Upton, New York 11973-5000, USA

Received: 15 August 2008 /
Published online: 6 December 2006 –

Abstract. Charged particle multiplicities in $A+A$ and $p(\bar{p})+p$ collisions as a function of pseudorapidity, centrality and energy are studied in both the nucleon and the constituent quark frameworks. In the present work, the calculation using the nuclear overlap model takes into account the fact that for the peripheral $A+A$ and $p+p$ collisions the number of nucleon and constituent quark participants cannot be smaller than two. A striking agreement is seen between the particle density in $A+A$ and $p(\bar{p})+p$ collisions, both at mid-rapidity and in the fragmentation regions, when normalized to the number of participating constituent quarks. The observations presented in this paper imply that the number of constituent quark pairs participating in the collision controls the particle production.

PACS. 25.75.-q; 25.75.Dw; 25.75.Nq; 24.10.Jv

1 Introduction

In this present work, I explore the implications of the picture in which the nucleon is viewed as a system of three clouds of partons, each containing a valence quark, a sea of quark–antiquark pairs, and gluons. In this picture, there are two length scales, that of the entire nucleon radius R_n, that determines the mean distance between the constituent quarks, and the proper radius of the constituent, r_q. Some QCD calculations of the nucleon spatial structure [1] support the description of three sub-objects of size 0.1–0.3 fm. Similar descriptions of extended constituents have been applied in energy-loss models [2] describing multihadron production in different colliding systems.

In this paper, we consider a modified version of calculations of the number of nucleon and constituent quark participants. A general problem in the previous calculations [3–5] stems from the fact that in the nuclear overlap model in peripheral collisions, the number of nucleon and constituent quark participants ($\langle N^n_{\rm part}\rangle$ and $\langle N^q_{\rm part}\rangle$) can be smaller than two. This is so, since in the peripheral limit the overlap integral has a meaning of 1/2 times the probability to have $\langle N^n_{\rm part}\rangle = 2$. In the previous calculation [3–5], the problem can be found in the estimate of $\langle N^n_{\rm part}\rangle$ for peripheral $A+A$ collisions and in the calculation of the number of constituent quark participants for $p+p$ collisions. A similar problem with the calculation of $\langle N^n_{\rm part}\rangle$ for $d+$Au collisions using an optical approach has been reported by Kharzeev et al. [6]. The goal of the present paper is to study the charged particle multiplicities in nucleus–nucleus $(A+A)$ and nucleon–nucleon $(p(\bar{p})+p)$ collisions in both the nucleon and the constituent quark frameworks. The main focus is on the data from the relativistic heavy ion collider (RHIC) [7–14].

[a] e-mail: rachid.nouicer@bnl.gov

2 Calculation of the number of participants

The number of nucleon participants, denoted by $\langle N^n_{\rm part}\rangle$, and the number of constituent quark participants denoted by $\langle N^q_{\rm part}\rangle$, are estimated using the nuclear overlap model in a manner similar to that used in [3–5]. However, I introduce in the present work a modification of the calculation procedure taking into account that for the peripheral collisions $A+A$ and for $p+p$ collisions in both frameworks the $\langle N^n_{\rm part}\rangle$ and $\langle N^q_{\rm part}\rangle$ cannot be smaller than two. The nuclear density profile is thus assumed to have a Woods–Saxon form,

$$n_A(r) = \frac{n_0}{1+\exp[(r-R_n)/d]}, \tag{1}$$

where n_0 is the normal nuclear density, R_n is the nucleus radius, and d is a diffuseness parameter.

For nucleus–nucleus $(A+B)$ collisions, the number of nucleon participants, $\langle N^n_{\rm part}\rangle$, is in the present work calculated using the relation

$$N^n_{\rm part}|_{AB} = \int {\rm d}^2 s T_A(\mathbf{s}) P_{AB}(\mathbf{b}) \left\{1-\left[1-\frac{\sigma^{\rm inel}_{NN} T_B(\mathbf{s}-\mathbf{b})}{B}\right]^B\right\} + \int {\rm d}^2 s T_B(\mathbf{s}-\mathbf{b}) P_{AB}(\mathbf{b}) \left\{1-\left[1-\frac{\sigma^{\rm inel}_{NN} T_A(\mathbf{s})}{A}\right]^A\right\} \tag{2}$$

where $T(b) = \int_{-\infty}^{+\infty} \mathrm{d}z n_A(\sqrt{b^2+z^2})$ is the thickness function, and $P_{AB}(\mathbf{b})$ is defined by

$$P_{AB}(\mathbf{b}) = \frac{1}{1-\exp(-\sigma_{NN}^{\mathrm{inel}} T_{AB}(\mathbf{b}))}\,, \tag{3}$$

where $T_{AB}(\mathbf{b})$ is the overlap function defined as the product of the thickness functions of the colliding nuclei A and B, integrated over the two transverse dimensions:

$$T_{AB}(\mathbf{b}) = \int \mathrm{d}^2 s' T_A(\mathbf{s}') T_B(\mathbf{s}'-\mathbf{b})\,. \tag{4}$$

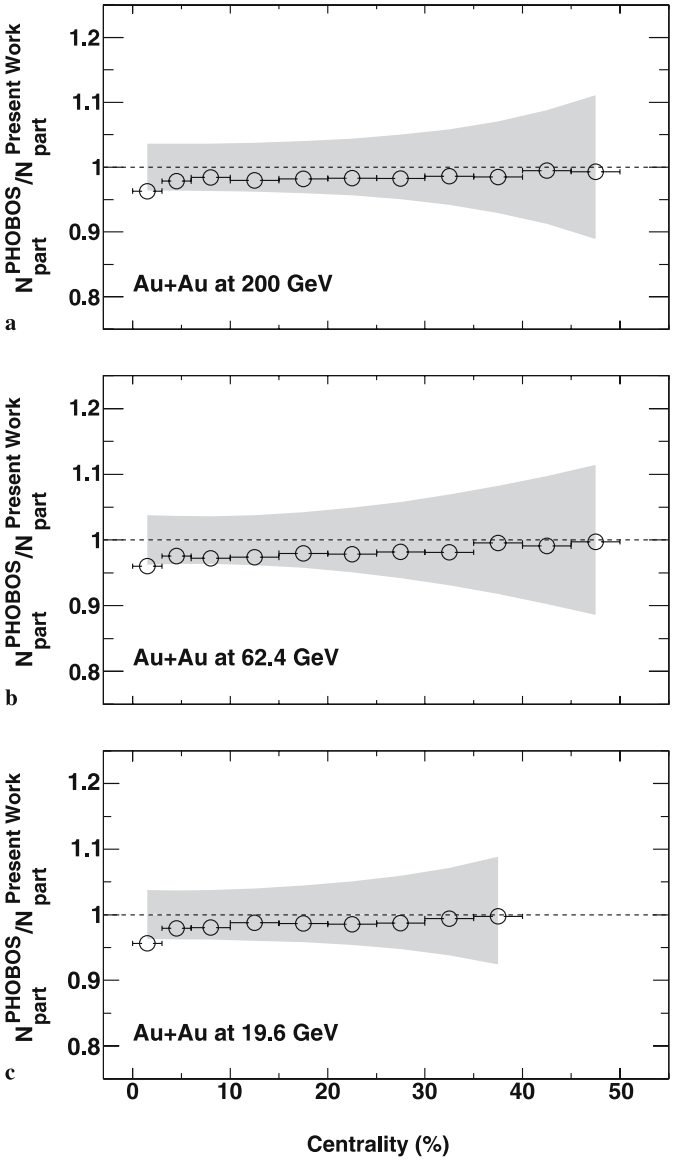

Fig. 1. Quantitative evaluation of the model calculations expressed as the ratio of the average number of nucleon participants of the PHOBOS Glauber calculations [17] to the present work as a function of centrality. Panel **a**–**c** correspond to Au+Au collisions at $\sqrt{s_{NN}} = 19.6$, 62.4 and 200 GeV, respectively. The *gray bands* correspond to the systematic errors on the $\langle N_{\mathrm{part}}^{n}\rangle$ of PHOBOS Glauber calculations

A and B are the mass numbers of the two colliding nuclei and $\sigma_{NN}^{\mathrm{inel}}$ is the inelastic nucleon–nucleon cross section. In the present work I use the FRITIOF parameterization $R_n = 1.16A^{1/3} - 1.16^2\mathrm{A}^{-}1/3$ fm and $d = 0.54$ fm which are well within the measurements of electron scattering from Au nuclei [15, 16].

Figure 1 shows the ratio of $\langle N_{\mathrm{part}}^{n}\rangle$ obtained by PHOBOS [17] and to the $\langle N_{\mathrm{part}}^{n}\rangle$ from the present work for Au+Au at $\sqrt{s_{NN}} = 19.6$, 62.4 and 200 GeV. The $\langle N_{\mathrm{part}}^{n}\rangle$ and $\langle N_{\mathrm{part}}^{q}\rangle$ from the present work are presented on Table 1 for Au+Au collisions at RHIC energies.

The number of constituent quark participants, $\langle N_{\mathrm{part}}^{q}\rangle$, is calculated in a similar manner by taking into account the following changes related to the physical realities and also taking into account that in peripheral collisions the number of $\langle N_{\mathrm{part}}^{q}\rangle$ cannot be smaller than two:

1. the density is three times that of the nucleon density with $n_0^q = 3n_0 = 0.51\ \mathrm{fm}^{-3}$;
2. the cross sections $\sigma_{CQ} = \sigma_{NN}^{\mathrm{inel}}/9$;
3. the mass numbers of the colliding nuclei are three times their values, keeping the size of the nuclei same as in the case of $\langle N_{\mathrm{part}}^{n}\rangle$.

Figure 2 presents the ratio of $\langle N_{\mathrm{part}}^{q}\rangle/\langle N_{\mathrm{part}}^{n}\rangle$ as a function of $\langle N_{\mathrm{part}}^{n}\rangle$ for Au+Au collisions at RHIC energies. The ratio shows that the correlation between $\langle N_{\mathrm{part}}^{n}\rangle$ and $\langle N_{\mathrm{part}}^{q}\rangle$ is not linear and that it depends on the colliding energy.

For proton–proton ($p+p$) collisions the same procedure has been used to calculate the number of constituent quark participants by using $A = 3$ and $B = 3$ and the nuclear density profile is assumed to have a sharp sphere form with uniform radii of 0.8 fm [18]. The reason to use sharp sphere density profile is because the Wood–Saxon density profile becomes unrealistic for low A. The systematic error related to this approximation can be estimated by running the code with $B = 1$ (for $p+A$), and comparing the obtained TAB(0) value with TA(0) (for impact parameter $b = 0$). The result is presented in Table 2. The discrepancy

Table 1. Numbers of constituent quark participants, $\langle N_{\mathrm{part}}^{q}\rangle$, obtained from the present work elucidated as a function of collision centrality in Au+Au collisions at $\sqrt{s_{NN}} = 19.6$, 62.4 and 200 GeV

Centrality (%)	200 GeV	62.4 GeV	19.6 GeV
Bin	$\langle N_{\mathrm{part}}^{q}\rangle$	$\langle N_{\mathrm{part}}^{q}\rangle$	$\langle N_{\mathrm{part}}^{q}\rangle$
0–3	952.5	907.2	869.4
3–6	837.7	796.0	761.4
6–10	731.4	693.1	661.8
10–15	614.5	580.4	552.8
15–20	501.7	472.1	448.4
20–25	408.5	382.9	362.7
25–30	331.6	309.7	292.6
30–35	265.3	246.8	232.4
35–40	209.1	193.5	181.6
40–45	161.6	148.8	139.1
45–50	123.1	112.8	105.1

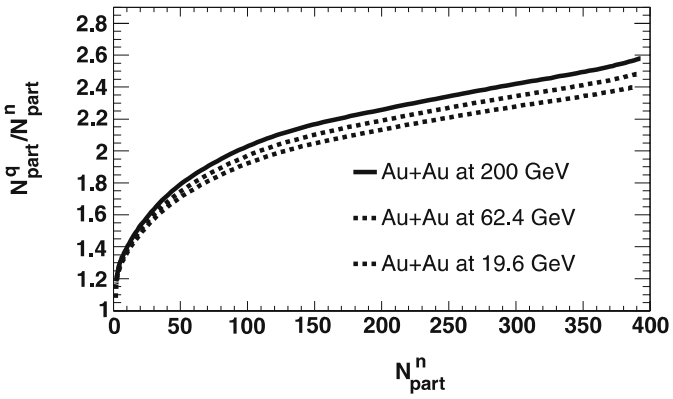

Fig. 2. Ratio of $\langle N^q_{\rm part}\rangle/\langle N^n_{\rm part}\rangle$ obtained from the present work presented as a function of the number of nucleon participants for Au + Au collisions at $\sqrt{s_{NN}} = 19.6$, 62.4 and 200 GeV

Table 2. Values of overlap function TAB and TA for impact parameter $b = 0$ calculated using densities profiles Wood–Saxon and sharp sphere for $p(A = 1) + B$ collisions using the nuclear overlap model

Profile	A	B	TAB(0)/TA(0)
Wood–Saxon	1	236	0.9
Wood–Saxon	1	12	0.6
Sharp sphere	1	236	1.0
Sharp sphere	1	12	0.9

Table 3. Values of $\langle N^q_{\rm part}\rangle$ obtained from the present work for most central and minimum-bias (min-bias) of $p(\bar{p}) + p$ collisions at several collisions energies

$\sqrt{s_{NN}}$ (GeV)	53	200	540	630	900	1800
$\sigma_{CQ} = \sigma_{NN}/9$	3.89	4.66	5.33	5.44	5.66	6.22
$\langle N^q_{\rm part}\rangle$(0%–6%)	4.37	4.94	5.46	5.55	5.72	5.98
$\langle N^q_{\rm part}\rangle$(min-bias)	3.10	3.29	3.47	3.51	3.57	3.73

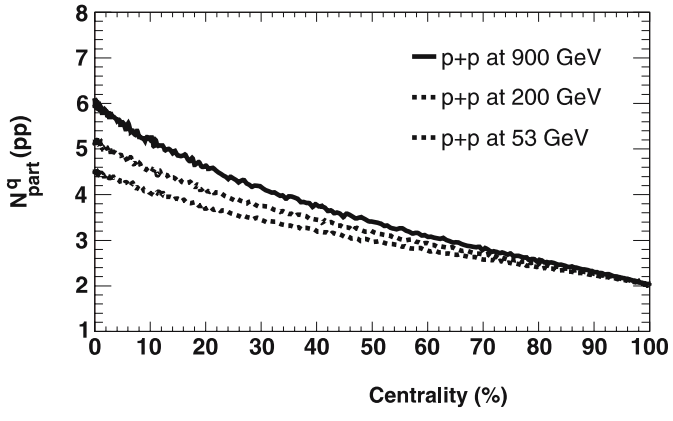

Fig. 3. Distributions of constituent quark participants $\langle N^q_{\rm part}\rangle$, obtained from the present work for $p+p$ at $\sqrt{s_{NN}} = 53$, 200, 900 GeV represented as a function of collisions centrality

is larger for a Wood–Saxon profile with low A. The $\langle N^q_{\rm part}\rangle$ for central, 0%–6%, and minimum bias of $p+p$ collisions are presented on Table 3. Figure 3 shows the distributions of the number of constituent quark participants obtained from the present work elucidated as a function of collisions centrality for nucleon–nucleon ($p+p$) collisions at $\sqrt{s_{NN}} = 53$, 200 and 900 GeV.

3 Physics results and discussions

Figure 4 shows the centrality dependence of the charged particle density per participant pair. Figure 4a shows the PHOBOS results [11, 17] on $\mathrm{d}N_{\rm ch}/\mathrm{d}\eta|_{|\eta|<1}$ per nucleon participant pair for Au + Au at 19.6, 62.4 and 200 GeV. The centrality dependence of the mid-rapidity yields has often been interpreted in a two component picture of particle production by soft and hard processes. As the beam energy increases, particle production from hard processes, which exceed the number of participants pairs by a factor ~ 5–6 in central events for $\sqrt{s_{NN}}$ ranging from 19.6 to 200 GeV, is expected to dominate over that from soft processes as the mini-jets cross sections increase [19]. Figure 4b shows the centrality dependence of $\mathrm{d}N_{\rm ch}/\mathrm{d}\eta|_{|\eta|<1}$ per constituent quark participants pair. I observe a constant or a slightly decreasing dependence of $(\mathrm{d}N/\mathrm{d}\eta)/(\langle N^q_{\rm part}\rangle/2)$ on centrality from peripheral to central collisions for Au + Au at 200 GeV and good scaling of $(\mathrm{d}N/\mathrm{d}\eta)/(\langle N^q_{\rm part}\rangle/2)$ on centrality for Au + Au at 19.6 and 62.4 GeV. In Fig. 4b, I extend the study presented in [5] from Au + Au at 200 GeV to 19.6 and 62.4 GeV using the new calculations. I agree with the interpretation presented in [5] that the experimentally observed increase of $(\mathrm{d}N_{\rm ch}/\mathrm{d}\eta|_{|\eta|<1})/(\langle N^n_{\rm part}\rangle/2)$ can be explained by the relative increase in the number of interacting constituent quarks in more central collisions. In the present work, I add to this study $\mathrm{d}N_{\rm ch}/\mathrm{d}\eta|_{|\eta|<1}$ of $p(\bar{p}) + p$ inelastic as well NSD collisions. In Fig. 4b, I observe that the $p(\bar{p}) + p$ data are in good agreement with Au + Au data for different collision centrality at the same energy. It should be noted that in Fig. 4b the $\mathrm{d}N_{\rm ch}/\mathrm{d}\eta|_{|\eta|<1}$ of $p(\bar{p}) + p$ data (open symbols) have been normalized by the minimum-bias $\langle N^q_{\rm part}\rangle$ presented in Table 3.

Figure 5 shows the primary charged particle density for central collisions at mid-rapidity divided by a) the number of participant nucleon pairs ($\langle N^n_{\rm part}\rangle/2$) as solid symbols and b) the number of participant constituent quark pairs ($\langle N^q_{\rm part}\rangle/2$) as open symbols presented as a function of collision energy.

The data are for Au + Au collisions at AGS, Pb + Pb collisions at the CERN-SPS [20–23] and for Au + Au and Cu + Cu collisions at RHIC [24]. Also shown for comparison are results from $p(\bar{p}) + p$ collisions [25].

In the nucleon participants framework (solid symbols in Fig. 5), the particle density per nucleon participant pair for $A + A$ collisions (solid points) shows an approximately logarithmic rise with $\sqrt{s_{NN}}$ over the full range of collision energies. The comparison of the particle density per nu-

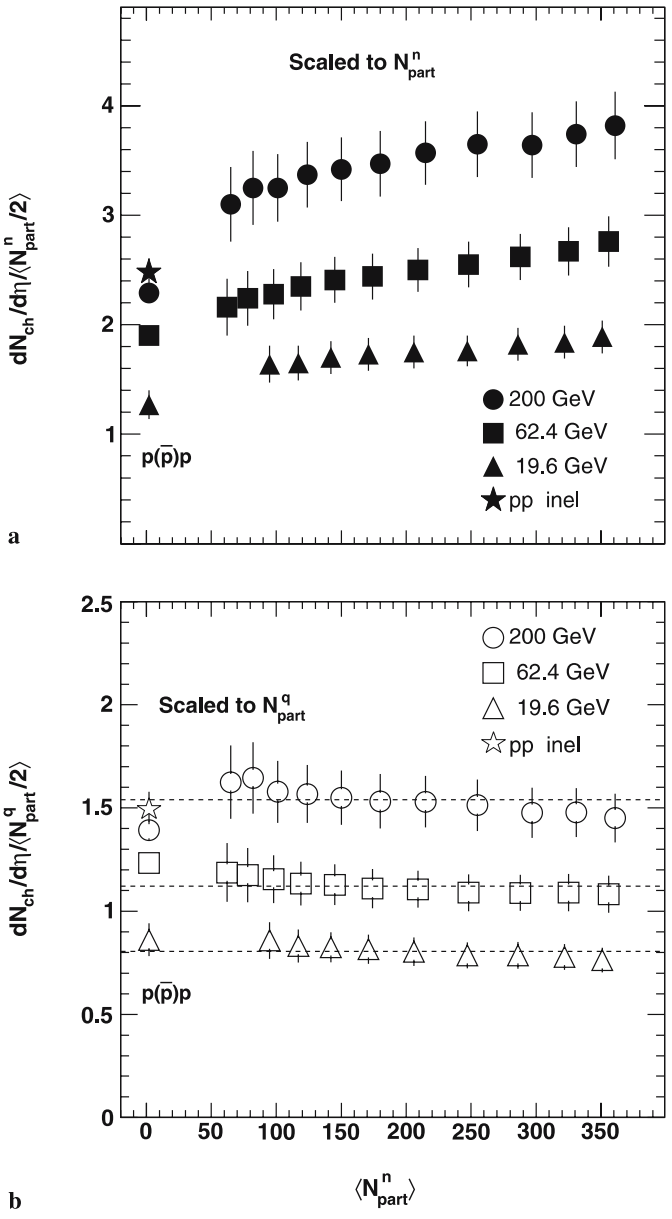

Fig. 4. Particle density, $\mathrm{d}N_{\mathrm{ch}}/\mathrm{d}\eta|_{|\eta|<1}$, divided by **a** the number of nucleon participants pairs, **b** the number of constituent quark participants pairs in Au + Au and $p(\bar{p})+p$ collisions at three energies [11, 17, 25]. The *dashed lines* in panel **b** correspond to the average of Au + Au data at given energy. The $p(\bar{p})+p$ for non-single diffractive (NSD) data are represented with similar symbols as Au + Au collisions at the same energy at $\langle N^n_{\mathrm{part}}\rangle = 2$. The *star symbols* in panel **a** and **b** correspond to $p(\bar{p})+p$ inelastic data at $\sqrt{s_{NN}} = 200$ GeV. The $p(\bar{p})+p$ data in in panel **b** have been normalized by the minimum-bias $\langle N^q_{\mathrm{part}}\rangle$

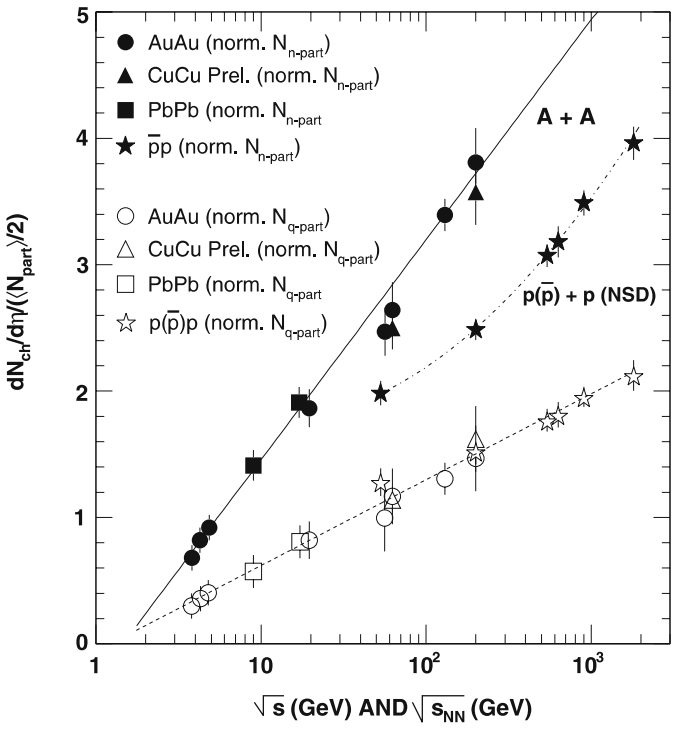

Fig. 5. Particle density per constituent quark participant pair (*open symbols*) and particle density per nucleon participant pair (*solid points*) produced in central (0%–6%) nucleus–nucleus ($A+A$) collisions presented as a function of collision energy at AGS, SPS [20–23] and RHIC [24] and in $p(\bar{p})+p$ collisions (inelastic) [25]. The *errors bars* correspond to the systematic errors. The *solid line* represents a linear fit through solid symbols for $A+A$ data, $f_{AA} = -0.287 + 0.757\ln(\sqrt{s})$. The *dashed dotted line* corresponds to the fit through *solid symbols* of $p(\bar{p})+p$ collisions, $f_{pp} = 2.25 - 0.41\ln(\sqrt{s}) + 0.09\ln^2(\sqrt{s})$. The *dashed line* corresponds to a linear fit trough the *open symbols* in the constituent quarks framework, $f_{p(\bar{p})p/AA} = -0.06 + 0.3\ln(\sqrt{s})$. It should be noted that the $\mathrm{d}N_{\mathrm{ch}}/\mathrm{d}\eta|_{|\eta|<1}$ of $p(\bar{p})+p$ data (*open symbols*) have been normalized by minimum-bias $\langle N^q_{\mathrm{part}}\rangle$ presented in Table 3

cleon of Au + Au to Cu + Cu collisions at the same energies, $\sqrt{s_{NN}} = 62.4$ and 200 GeV indicates that in symmetric nucleus–nucleus collisions the density per nucleon participant does not depend on the size of the two colliding nuclei but only on the collision energy. This means that for Si + Si collisions at $\sqrt{s_{NN}} = 200$ GeV, the particle density per nucleon participant will be similar to Au + Au collisions at the same energy. Also I observe that the charged particle multiplicity per participant nucleon pair (solid symbols) in $A+A$ collisions is higher compared to $p(\bar{p})+p$ collisions at the same energy. It should be noted that the number of nucleon participants for $p(\bar{p})+p$ has been chosen to be $2(\langle N^n_{\mathrm{part}}\rangle(pp) = 2)$.

In contrast, I observe that the particle density per constituent quark participant pair (open symbols in Fig. 5) is similar for nucleus–nucleus collisions and nucleon–nucleon collisions at the same energy. It thus appears that using partonic participants accounts for the observed multiplicity in both $A+A$ and $p(\bar{p})+p$ collisions. It should be noted that Fig. 5 is similar to Fig. 6 presented in [3], but it was done independently, extended to the Cu + Cu system, and used the new version of calculation as presented in this paper.

Figure 6 shows the integrated total charged particle divided by a) per nucleon participant pair $(N_{\mathrm{ch}}/(\langle N^n_{\mathrm{part}}\rangle/2))$, b) per constituent quarks participant pair $(N_{\mathrm{ch}}/(\langle N^q_{\mathrm{part}}\rangle/2))$

for Au + Au and $p(\bar{p})+p$ collisions at the same energy, 200 GeV.

In the nucleon participant framework, panel a), the integrated total charged particle in Au + Au collisions, as a function of number nucleon participants, is higher than $p(\bar{p})+p$ collisions, indicating that there is no smooth transition between $A+A$ and nucleon–nucleon collisions [14]. This observation can be strongly confirmed by adding the preliminary data from Cu + Cu presented by PHOBOS collaboration [24] (not shown in this figure) which correspond to the peripheral data of the Au + Au system at the same energy. These comparisons between $A+A$ and $p(\bar{p})+p$ collisions are, however, based on scaling with the number of nucleon participants. In the constituent quarks framework, panel b), the $N_{\rm ch}/(\langle N^q_{\rm part}\rangle/2)$ of $p+p$ NSD (or inelastic) collisions agree with the central Au + Au collisions at the same energy.

In general, the charged particle production in the fragmentation region is thought to be distinct from that at mid-rapidity, although there is no obvious evidence for two separate regions at any of the RHIC energies. This observation is made based on the $\mathrm{d}N_{\rm ch}/\mathrm{d}\eta$ distributions of charged particle presented in [13, 26]. Figure 7 shows the charged particles produced in the fragmentation region for the most central (0%–6%) Au + Au collisions at four RHIC energies compared to $p(\bar{p})+p$ (inelastic and (NSD)) collisions at 200 GeV. When normalized to $\langle N^n_{\rm part}\rangle/2$, Fig. 7a, I observe that the multiplicity in the limiting fragmenta-

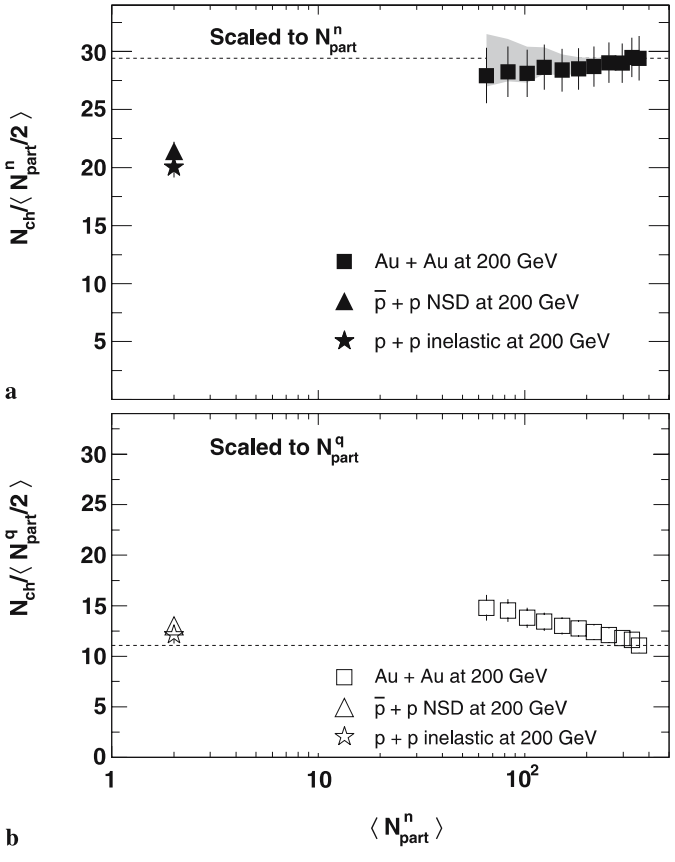

Fig. 6. Integrated total charged particles obtained from Au + Au collisions and $p(\bar{p})+p$ inelastic as well NSD collisions at the same energy $\sqrt{s_{NN}} = 200$ GeV [11, 17, 25] normalized by **a** number of nucleon participant pairs, **b** number of constituent quarks participant pairs. The errors shown with *vertical bars* are full systematic errors. In panel **b** $N_{\rm ch}$ for $p(\bar{p})+p$ data (*open symbols*) have been normalized by minimum-bias $\langle N^q_{\rm part}\rangle$. The *dashed lines* are guide lines relatively to the most central collisions in Au + Au system

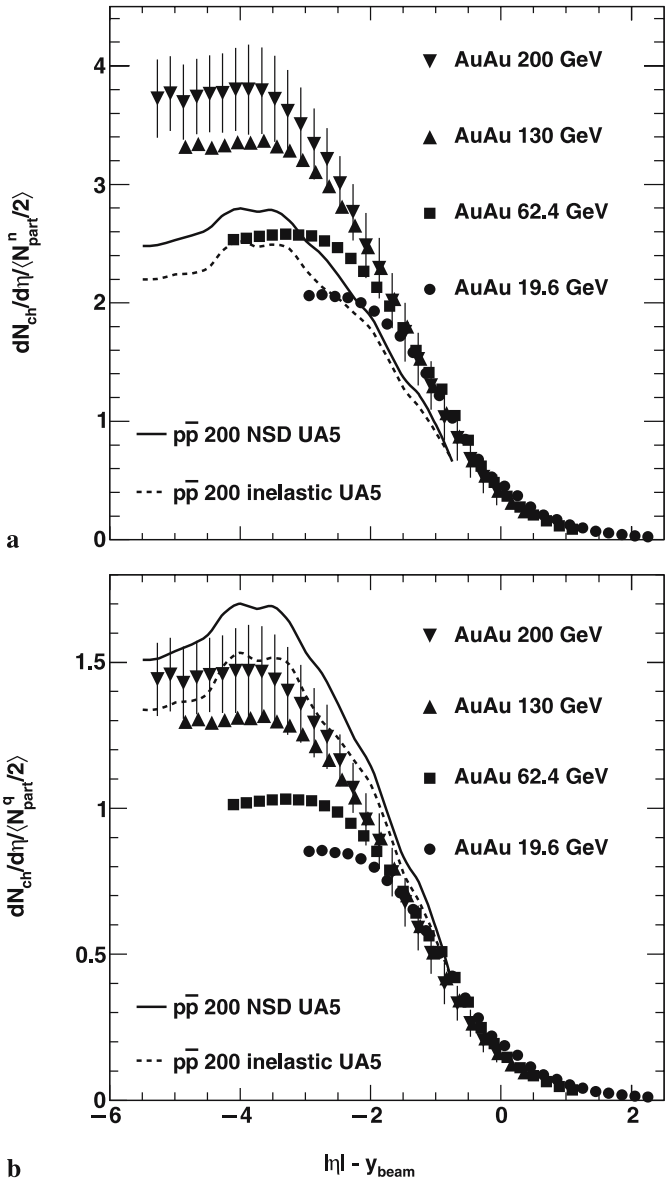

Fig. 7. Pseudorapidity distributions of charged particle for Au + Au collisions at RHIC energies [11] and $p(\bar{p})+p$ collisions at 200 GeV [25]. The distributions have been shifted to $\eta - y_{\rm beam}$ in order to study the fragmentation regions in one of the nucleus rest frame. Panels **a** and **b** correspond to $\mathrm{d}N_{\rm ch}/\mathrm{d}\eta$ distributions scaled to the number on nucleon participants pairs and to the number of constituent quark participants pairs, respectively. The systematic errors have been shown just for Au + Au at 200 GeV for clarity. In panel **b** the $p(\bar{p})+p$ data have been normalized by the minimum-bias $\langle N^q_{\rm part}\rangle$

tion region in $A+A$ collisions is higher than for $p(\bar{p})+p$ collisions at the same energy, $\sqrt{s_{NN}}$=200 GeV. If, however, the comparison is carried out for multiplicities normalized to $\langle N^q_{\rm part}\rangle/2$, Fig. 6b, $A+A$ and $p(\bar{p})+p$ collisions exhibit a striking degree of agreement. Again, this observation implies that the number of constituent quark pairs participating in the collision controls the particle production in the central collisions.

4 Conclusions

The charged particle production results from $A+A$ and $p(\bar{p})+p$ collisions have been compared based on the number of nucleon participants and the number of constituent quark participants. In both normalizations, I observe that the charged particle densities in Au + Au and Cu + Cu collisions are similar for both $\sqrt{s_{NN}} = 62.4$ and 200 GeV. This implies that in symmetric nucleus–nucleus collisions the charged particle density does not depend on the size of the two colliding nuclei but only on the collision energy. In the nucleon participants framework, the particle density at mid-rapidity as well as in the fragmentation region from $A+A$ collisions are higher than those of $p(\bar{p})+p$ collisions at the same energy. Also the multiplicity of total charged particle, in $A+A$ collisions, as a function of number nucleon participants is higher than $p(\bar{p})+p$ collisions at the same energy indicating that there is no smooth transition between peripheral $A+A$ and nucleon–nucleon collisions. However, when the comparison is made in the constituent quarks framework, $A+A$ and $p(\bar{p})+p$ collisions exhibit a striking degree of agreement. The observations presented in this paper imply that the number of constituent quark pairs participating in the collision controls the particle production.

Acknowledgements. I would like to express my gratitude to Bhaskar De for making his code available for a cross-check. I would also like to express my gratitude to S. Eremin and S. Voloshin, and I thank D. Miskowiec for making his code "nuclear ovelap model" available. Also I would like to thank M.D. Baker and B. Wosiek for valuable advice concerning the present work. This work was supported by U.S. DOE Grant No. DE-AC02-98CH10886.

References

1. E. Shuryak, Phys. Lett. B **496**, 378 (2000)
2. E.K.G. Sarkisyan et al., American Institute of Physics Conf. Proc. **828**, 35 (2006)
3. B. De et al., Phys. Rev. C **71**, 024 903 (2005)
4. R. Nouicer, American Institute of Physics Conf. Proc. **828**, 11 (2006)
5. S. Eremin et al., Phys. Rev. C **67**, 064 905 (2003)
6. D. Kharzeev et al., Nucl. Phys. A **730**, 448 (2004)
7. I. Arsene et al., Nucl. Phys. A **757**, 1 (2005)
8. K. Adcox et al., Nucl. Phys. A **757**, 184 (2005)
9. B.B. Back et al., Nucl. Phys. A **757**, 28 (2005)
10. J. Adams et al., Nucl. Phys. A **757**, 102 (2005)
11. B.B. Back et al., arXiv:nucl-ex/0509034
12. B.B. Back et al., Phys. Rev. Lett. **88**, 22 302 (2002)
13. PHOBOS Collaboration, R. Nouicer et al., arXiv:nucl-ex/0601026
14. B.B. Back et al., Phys. Rev. C **72**, 031 901(R) (2005)
15. B. Hahn et al., Phys. Rev. **101**, 1131 (1956)
16. C.W. De Jager et al., Atom. Data Nucl. Data **24**, 479 (1974)
17. B.B. Back et al., Phys. Rev. C **70**, 021 902(R) (2004)
18. C.Y. Wong, World Sci., **161**, (1994)
19. M. Gyulassy et al., Comput. Phys. Commun. **83**, 307 (1994)
20. L. Ahle et al., Phys. Lett. B **476**, 1 (2000)
21. L. Ahle et al., Phys. Lett. B **490**, 53 (2000)
22. J. Bachler et al., Nucl. Phys. A **661**, 45 (1999)
23. C. Blume et al., Proc. QM (2001)
24. PHOBOS Collaboration, G. Roland et al., arXiv:nucl-ex/0510042
25. F. Abe et al., Phys. Rev. D **41**, 2330 (1990)
26. B.B. Back et al., Phys. Rev. Lett. **91**, 052 303 (2003)